

Status of the ATLAS Liquid Argon Calorimeter and its performance after one year of LHC operation

L. March (UAM-Madrid)

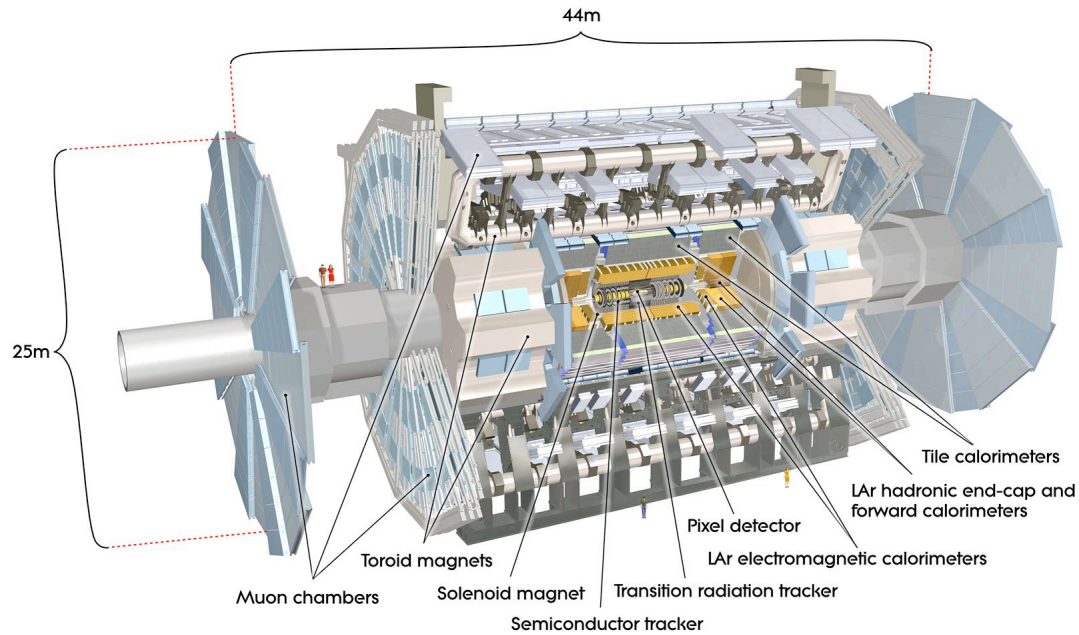
on behalf on the ATLAS Liquid Argon Calorimeter Group

(IEEE) High energy physics and nuclear physics detectors: Calorimeters

27th October, Valencia (Spain)

Overview of the ATLAS Liquid Argon (LAr) calorimeters

A Toroidal LHC Apparatus (ATLAS) detector



Structure:

Tracking: Pixel, Silicon detector and Transition Radiation Tracker; in a solenoidal magnetic field

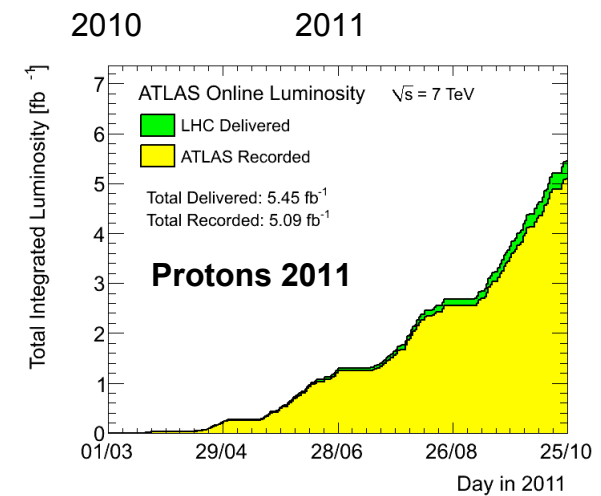
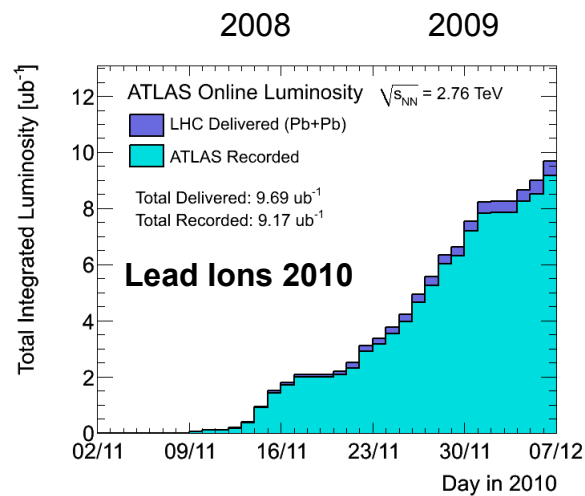
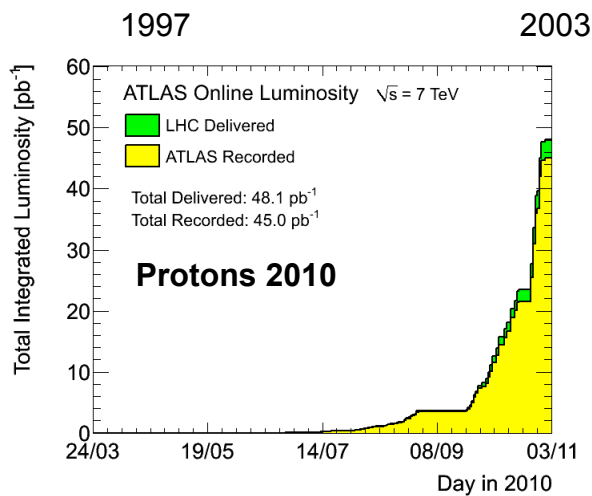
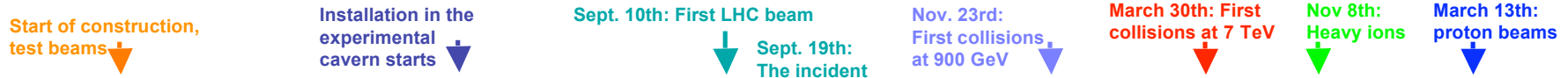
Calorimetry:

- Electromagnetic: LAr in endcaps and barrel
- Hadronic: Scintillators in barrel

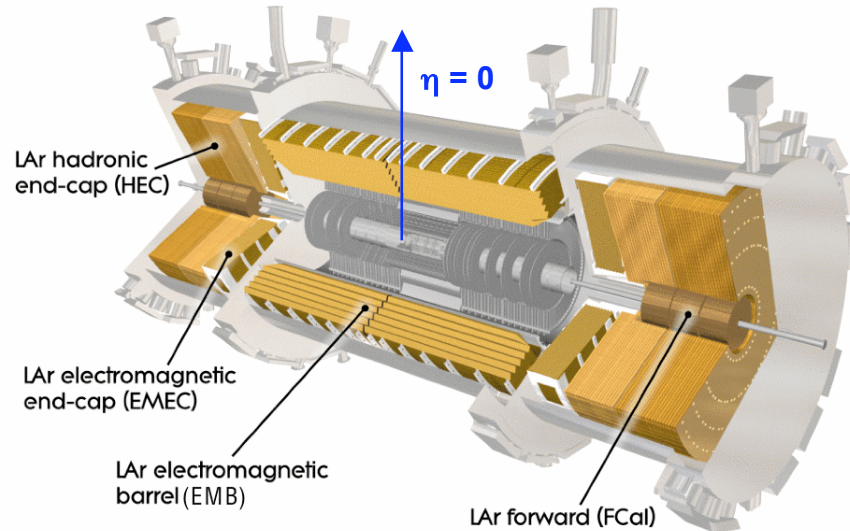
Muon Spectrometer: Drift Chambers, Resistive Plate Chambers; in a toroidal magnetic field

Physics goals:

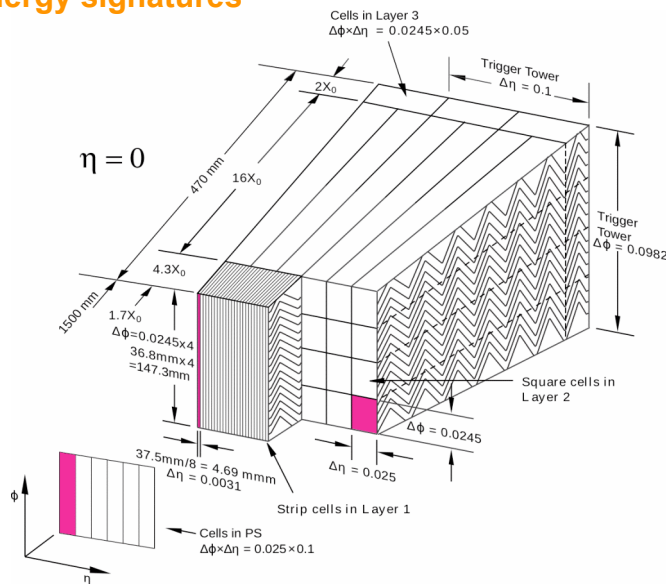
Precision Electroweak measurements, Higgs, Physics Beyond Standard Model



ATLAS Liquid Argon (LAr) Calorimeters



LAr calorimeters play a central role in ATLAS detector. They measure energies of electrons and photons with high resolution and detect hadronic jets and missing energy signatures



Electromagnetic Calorimeter (EM)

Absorber: Pb & active medium: LAr

Accordion geometry: full ϕ coverage

Coverage: $|\eta| < 3.2$

Design resolution: $\frac{\Delta E}{E} = \frac{10\%}{\sqrt{E(\text{GeV})}} \oplus 0.7\%$

3 layers up to $|\eta| = 2.5$; 2 up to $|\eta| = 3.2$

Presampler up to $|\eta| = 1.8$

173312 readout channels (99.8 % operational)

Forward Calorimeter (FCal)

Cu/W tubes & LAr

Coverage: $3.1 < |\eta| < 4.9$

Design resolution: $\frac{\Delta E}{E} = \frac{100\%}{\sqrt{E(\text{GeV})}} \oplus 10\%$

1 EM, 2 hadronic layers

3524 readout channels (99.8 % operational)

Hadronic EndCap Calorimeter (HEC)

Cu & LAr

Coverage: $1.5 < |\eta| < 3.2$

Design resolution: $\frac{\Delta E}{E} = \frac{50\%}{\sqrt{E(\text{GeV})}} \oplus 3\%$

4 layers

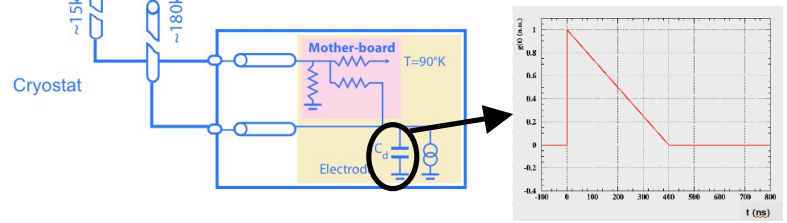
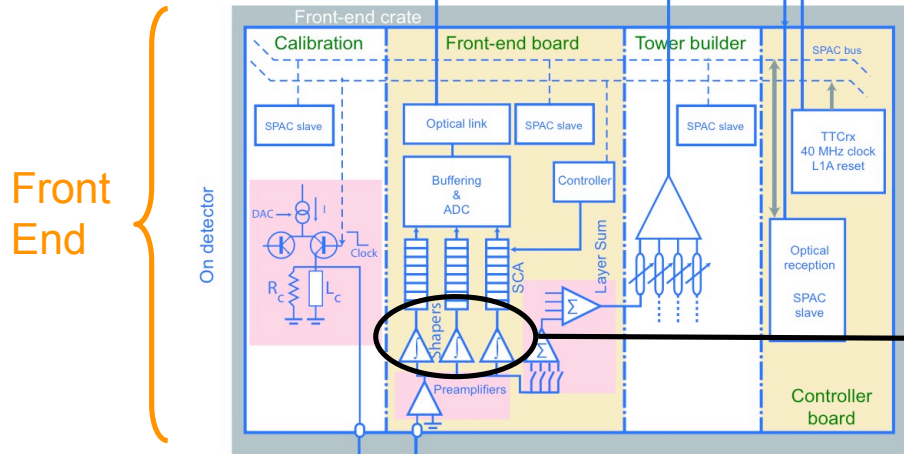
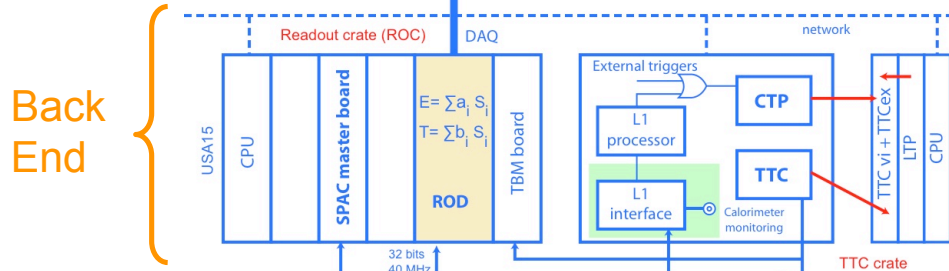
5632 readout channels (99.6 % operational)

Signal reconstruction

$$A = \sum_{i=1}^{N_{samples}} a_i (s_i - p)$$

$$\tau = \frac{1}{A} \sum_{i=1}^{N_{samples}} b_i (s_i - p)$$

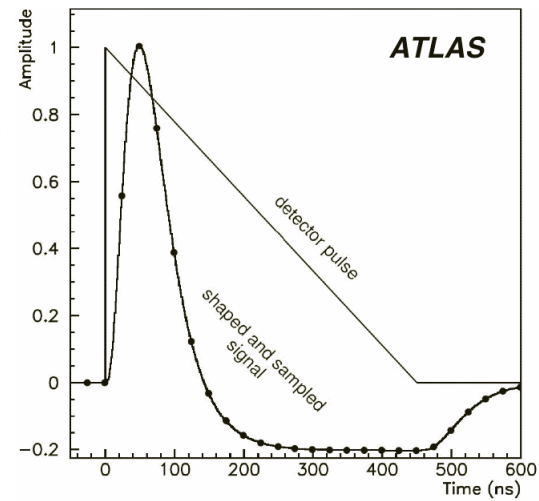
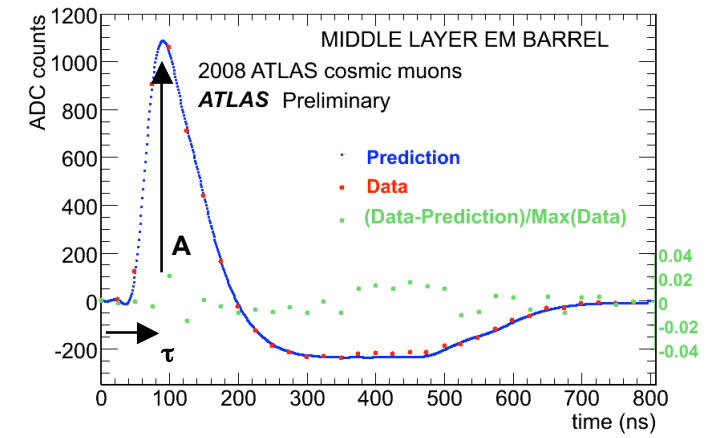
s_i ≡ Sample ADC counts
 a_i, b_i ≡ Optimal Filtering Coefficients
 p ≡ pedestal



Shaped signal, sampled at 40 MHz, digitized

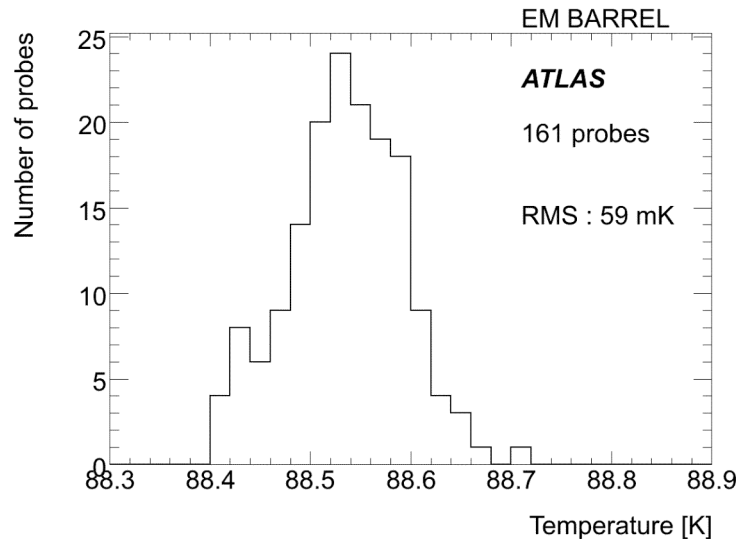
Shaping: 3 gains (MeV to TeV)

Ionization pulse



LAr detector operation

Detector operation (1)

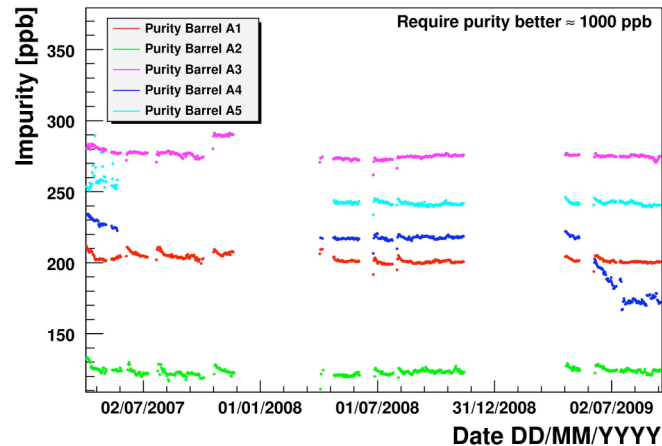


LAr temperature stability

59 mK RMS

- Excellent homogeneity and stability for LAr temperature
- Each cryostat: ~ 88 K
- Designed value of < 100 mK for stability
- Signal sensitivity to temperature change: 2% / K

Purity Barrel Side A



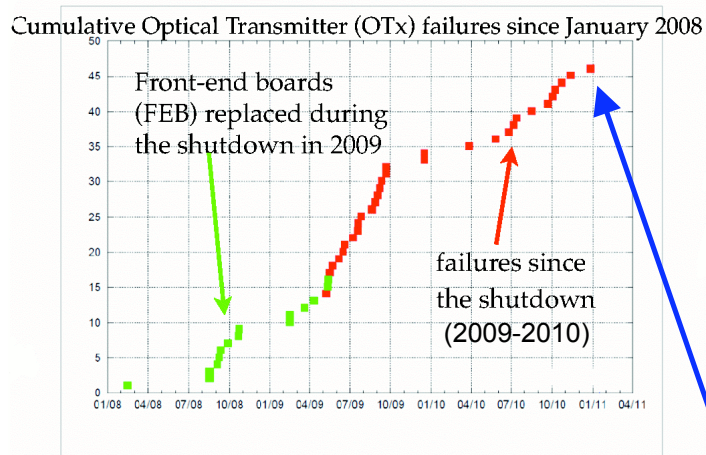
LAr purity in each cryostat is well within required limits

- Measured signal reduced by electronegative impurities
- Requirement: < 1000 ppb O₂ equivalent
- Measured with purity monitors:
Barrel ~ 200 ppb, EndCap ~ 140 ppb
- Impurity level in LAr is in the range of 200 ± 100 ppb

LAr temperature and impurity below requirements: negligible effect on constant term of the energy resolution

Problems: Optical Transmitter (OTx) deaths, High Voltage (HV) trips and Noise bursts

Detector operation (2)



1 Optical Transmitter (OTx) per Front-End Board (FEB) = 128 channels

OTx failure means no data is transmitted for entire FEB, but still have analogical readout through Level 1 Calo trigger connection

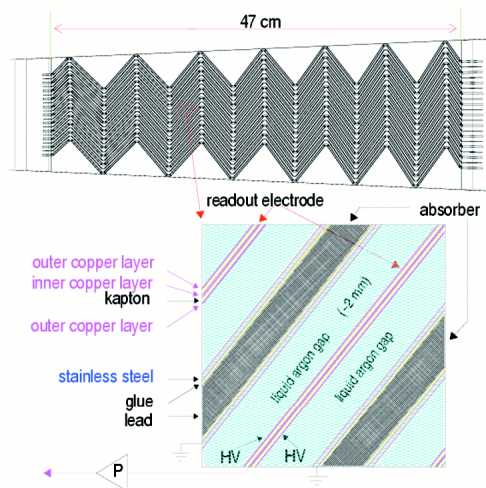
FEB replacement: Access not possible, except in periods of extended shutdown (Winter)

Became an issue in 2008, with 1 failure a week: Not definitely understood

Data analysis excluded affected regions (small detector acceptance loss: few % per electron)

No failures were reported since 2010-2011 shutdown exchange

The HV power supply system provides drift voltage across gaps in the calorimeter from back of the electrodes

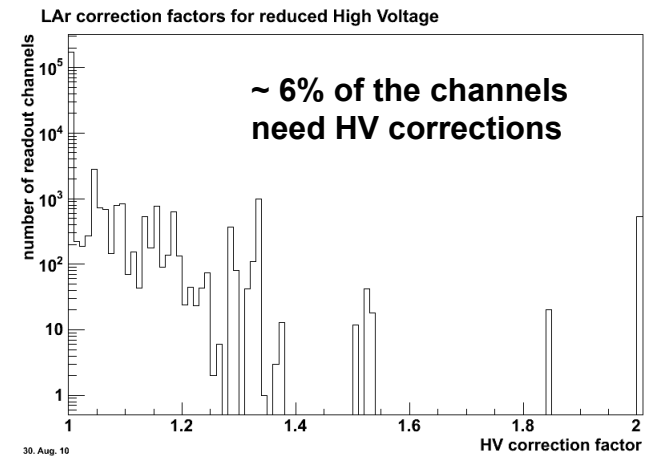


Each HV channel individually controlled (on/off, voltage, trip current, voltage ramp speed) by software

HV trips are observed and correlated with the presence of collisions

In a sequence of steady fills with the same luminosity / number of bunches, number of trips decreases with each fill

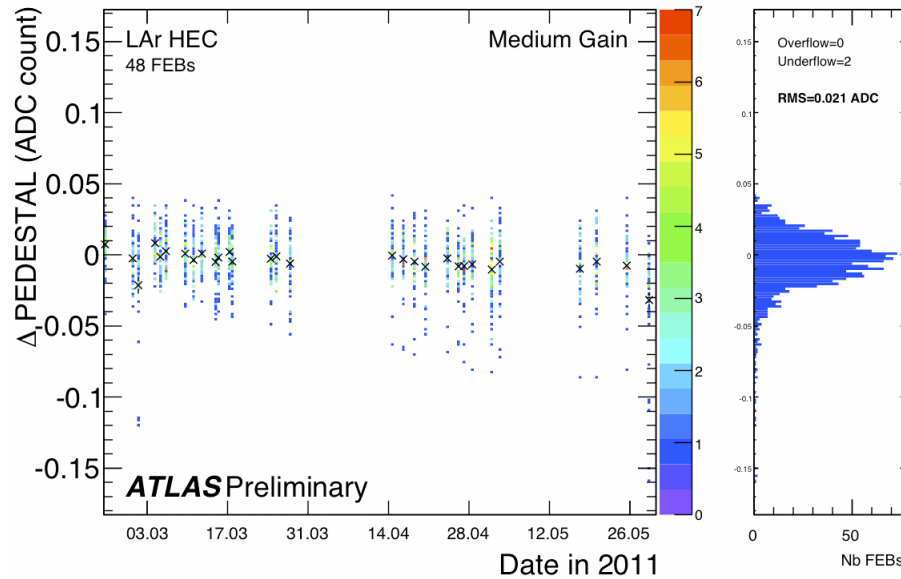
Automatic recovery procedure has been in use (data corrected for reduced HV during recovery, offline)



Noise bursts: Noise affecting a large number of channels in the same detector partition - are masked in data analysis

Performance of the LAr calorimeters

Stability of electronic calibration constants



Calibration runs are taken between every LHC fill

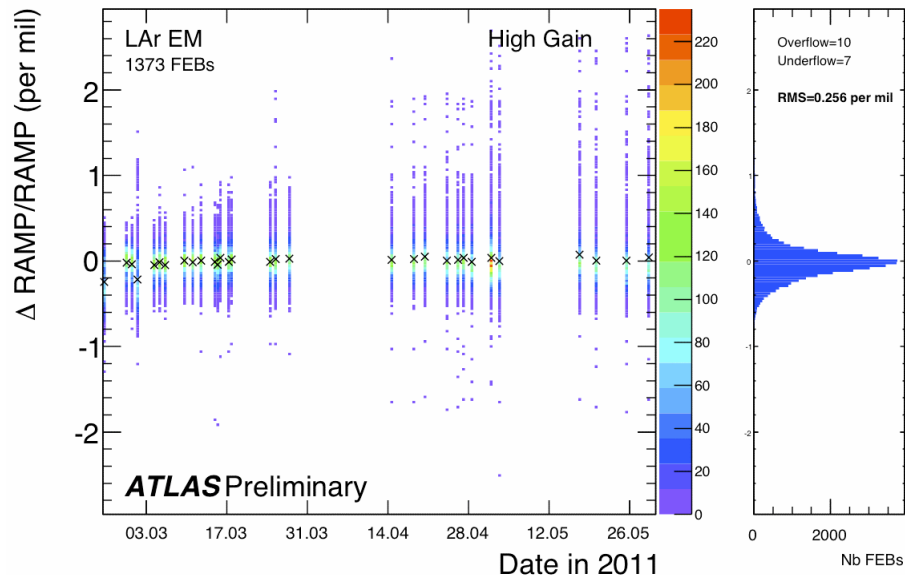
Calibration constants are updated every few weeks

Three kind of calibration runs for each gain:

1) Pedestal: response of the readout electronics without any injected signal into the LAr cells

2) Delay: response of each readout cell after amplification and shaping

3) Ramp: response of each cell as a function of the injected current



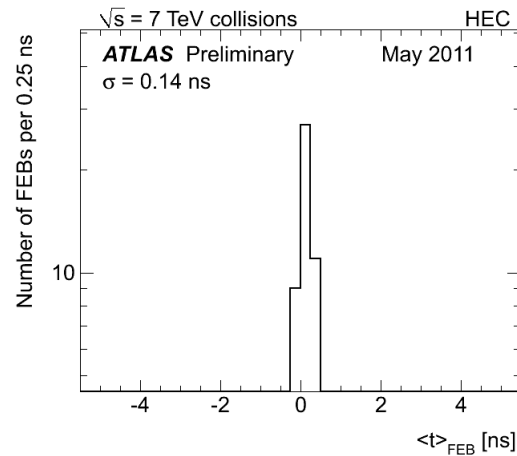
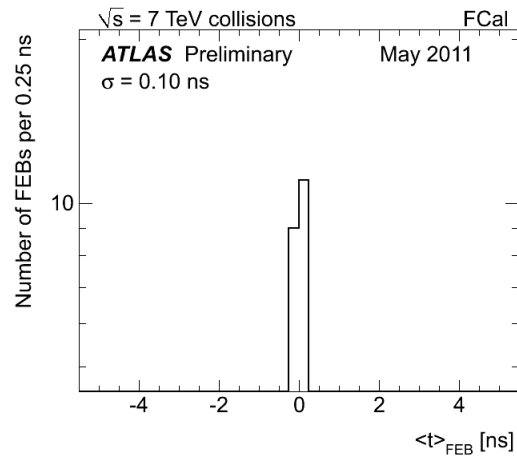
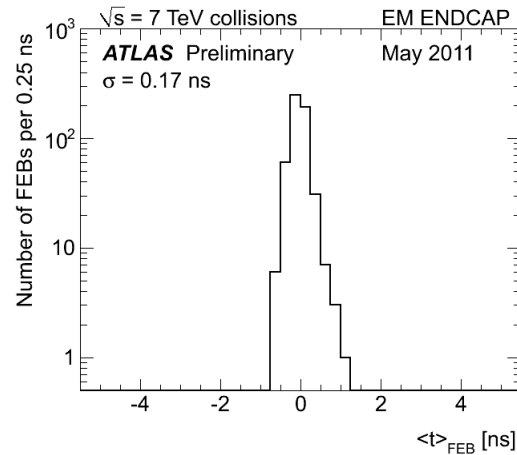
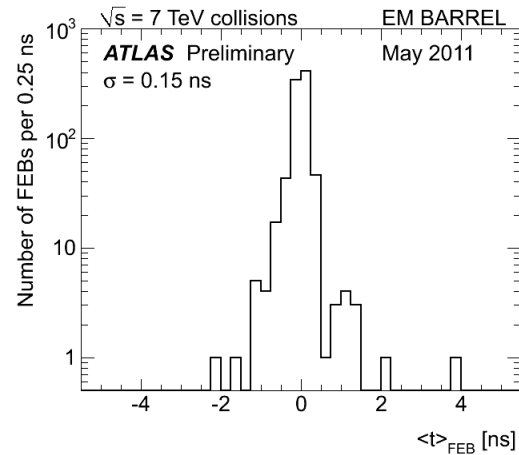
Stability constants is monitored over long periods

Pedestal change by ADC counts:
< 0.03 for all calorimeters (< 3 MeV)

Ramp change: < 0.1 % for all calorimeters

Well established and robust calibration procedure and very good electronics stability

Timing alignment



Synchronize readout clock with bunch crossings

$\langle t \rangle_{\text{FEB}}$ = difference between measured and predicted delay (averaged over 128 channels of each Front-End Boards (FEB))

Predict delay due to cabling and time of flight

Compute time from collision data

Good understanding of the timing helps distinguish between energy deposited from triggered events and those from neighbouring bunch crossings

Used to veto cosmic against collision events

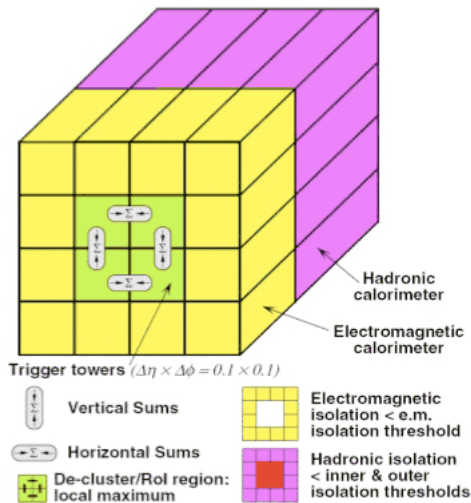
The depth segmentation and timing can also be used together to identify non-pointing photons.

Coarse adjustment achieved with configurable delays on the Front-End Boards

Finer adjustments can be made channel-by-channel with optimal filtering coefficients

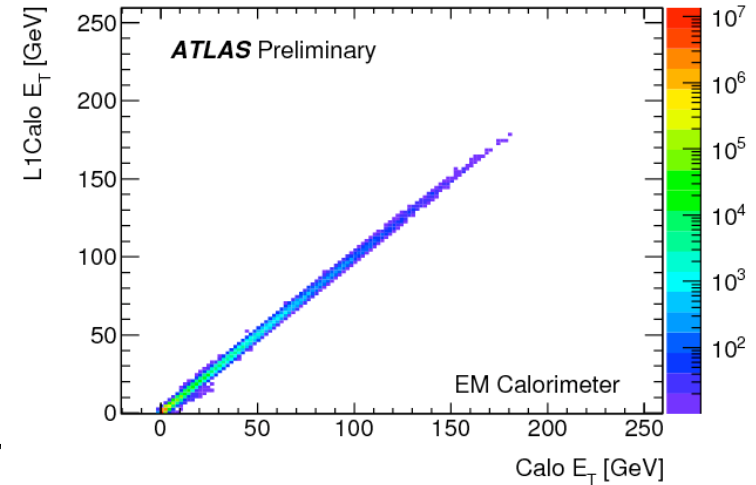
The ultimate goal is a timing resolution of $\sim 100 \text{ ps}$

Performance of LAr trigger



Same detector
 Different readout
 Coarser granularity
 Comparison with
 offline LAr transverse
 energy

Energy correlation (Beginning of 2011)



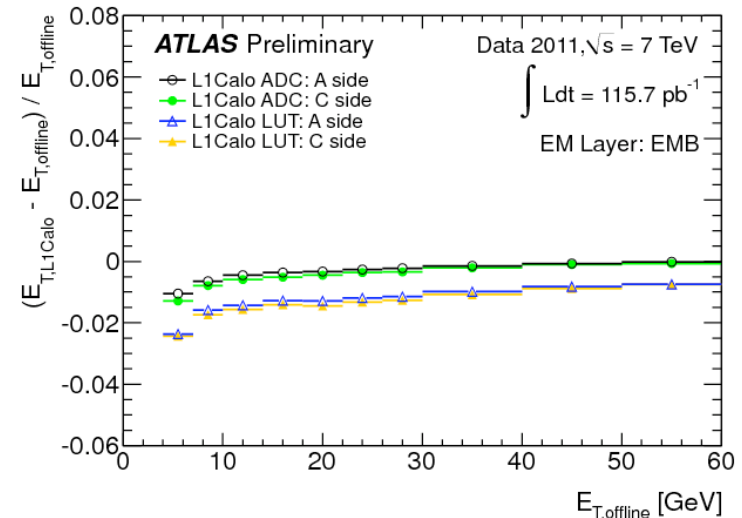
Energy is summed over neighbouring cells in the trigger tower

Typical size: $\Delta\eta \times \Delta\phi = 0.1 \times 0.1$
 (approx. 60 readout channels)

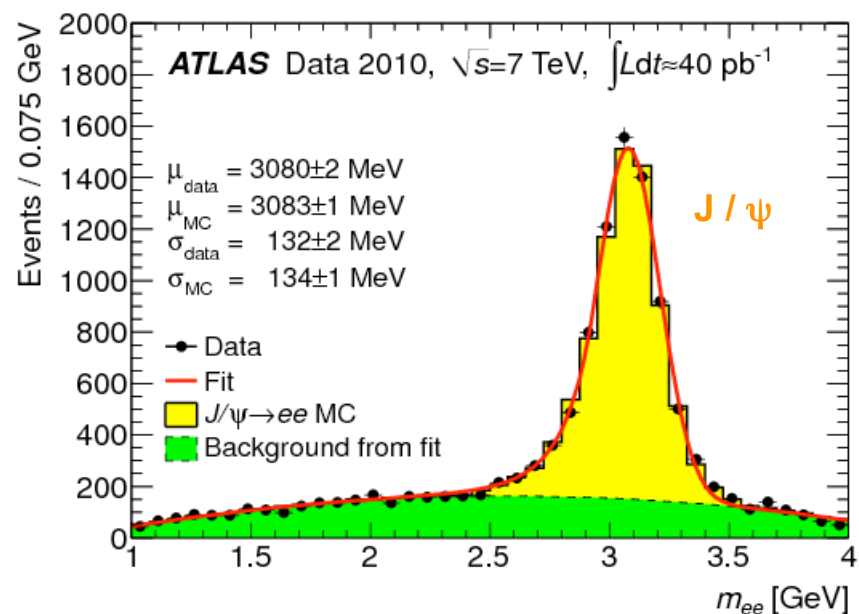
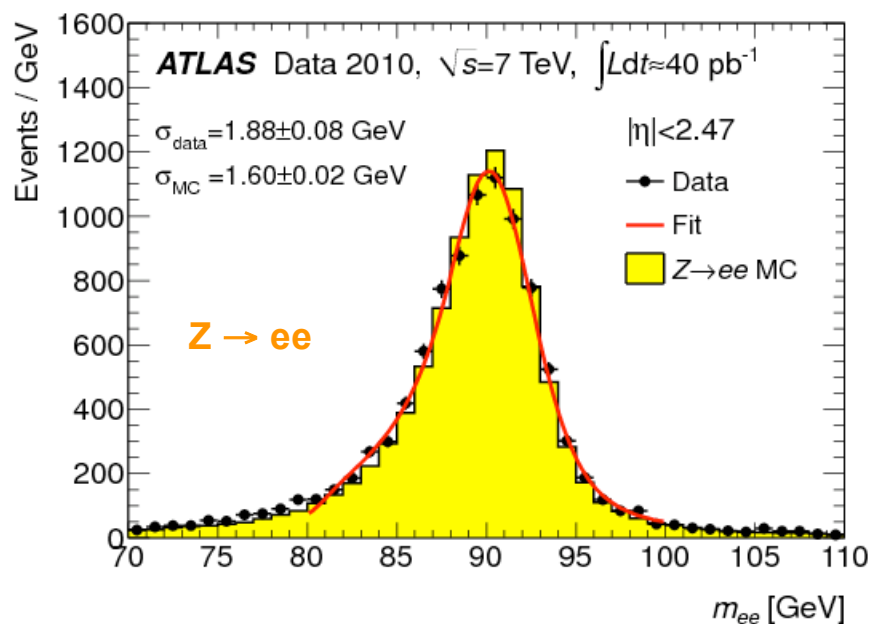
Trigger energy can be used to correct energy when digital readout is missing

Resolution of E_T (L1Calo) $< 5\%$
 (design resolution constant term at high energy) for $E_T(\text{LAr}) > 10$ GeV

Energy resolution (Early 2011)



Performance of LAr detectors

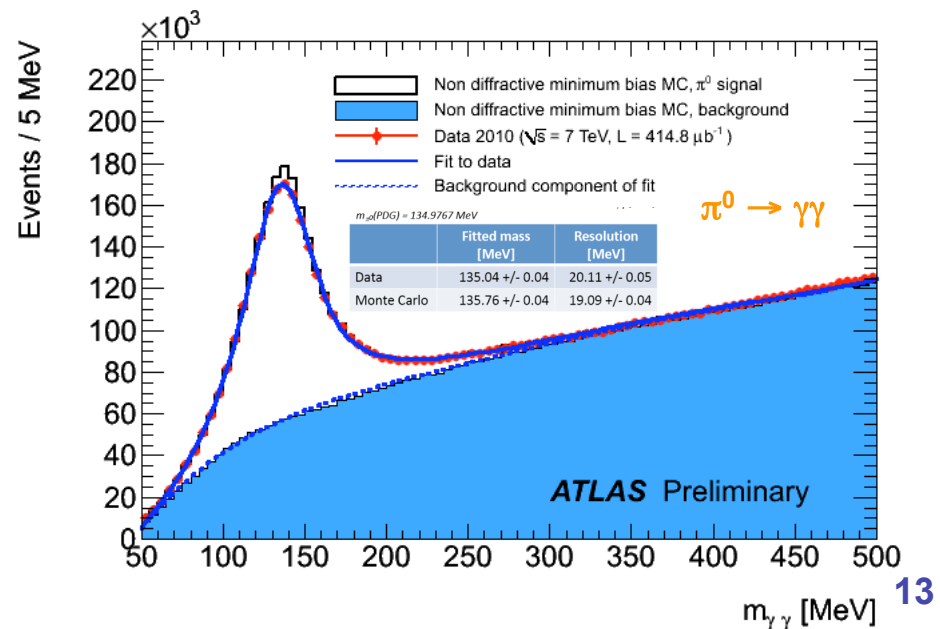


Electromagnetic energy scale and uniformity:

- Calibration signals and physics signals
- $Z \rightarrow ee$ events for high-pt electrons
- $J/\psi \rightarrow ee$ for low-pt electron, π^0 decays

γ/π^0 separation based on the width of the shower

Good detector performance for physics analysis



Summary and conclusions

ATLAS LAr Calorimeter is fully instrumented and has been operated at nominal high voltage since 2006

It measures the energy and direction of electrons, photon, jets, E_T^{miss} of events with high precision

LAr Calorimeter is well understood, the performance of the calorimeter is excellent, near design expectations

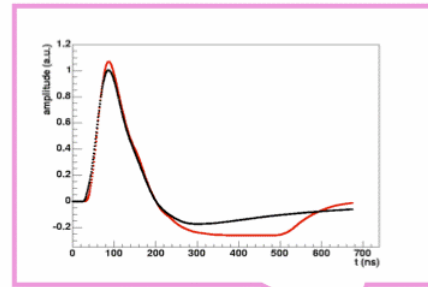
Few occasional problems encountered in the past year (failures of optical transmitters and high voltage power supply trips) are mitigated in the detector operations and data analysis

Problems solved or worked on

We are entering an exciting period and are prepared for a large amount of data and increased luminosity

Back-up slides

Energy reconstruction



$$E_{\text{cell}} = F_{\mu\text{A} \rightarrow \text{MeV}} \cdot F_{\text{DAC} \rightarrow \mu\text{A}} \cdot \frac{1}{\frac{M_{\text{phys}}}{M_{\text{cali}}}} \sum_{i=1}^{M_{\text{ramps}}} R_i \left[\sum_{j=1}^{N_{\text{samples}}} a_j (s_j - p) \right]^i$$

Cell energy
Sampling fraction
Calibration board
ADC to DAC (Ramps)
Pulse Samples
Optimal Filtering Coefficients
Pedestals

The above formula describe the LAr electronic calibration chain (from the signal ADC samples to the raw energy in the cell). Note that this version of the formula uses the general M_{ramps} -order polynomial fit of the ramps. Actually we just use a linear fit (electronic is very linear, and additionally we only want to apply a linear gain in the DSP in order to be able to undo it offline, and apply a more refined calibration). In this case, the formula is simply:

$$E_{\text{cell}} = F_{\mu\text{A} \rightarrow \text{MeV}} \cdot F_{\text{DAC} \rightarrow \mu\text{A}} \cdot \frac{1}{\frac{M_{\text{phys}}}{M_{\text{cali}}}} \cdot R \left[\sum_{j=1}^{N_{\text{samples}}} a_j (s_j - p) \right]$$